Pharmacokinetics and Biodistribution of Novel Aptamer Compositions

Judith M. Healy,[1] Scott D. Lewis,[1] Markus Kurz,[1] Ryan M. Boomer,[1] Kristin M. Thompson,[1] Charles Wilson,[1] and Thomas G. McCauley[1,2]

Received April 20, 2004; accepted August 10, 2004

Purpose. Aptamers are highly selective nucleic acid–based drugs that are currently being developed for numerous therapeutic indications. Here, we determine plasma pharmacokinetics and tissue distribution in rat of several novel aptamer compositions, including fully 2′-*O*-methylated oligonucleotides and conjugates bearing high-molecular weight polyethylene glycol (PEG) polymers, cell-permeating peptides, and cholesterol.

Methods. Levels of aptamer conjugates in biological samples were quantified radiometrically and by a hybridization-based dual probe capture assay with enzyme-linked fluorescent readout. Intact aptamer in urine was detected by capillary gel electrophoresis and matrix-assisted laser desorption ionization time of flight mass spectrometry (MALDI-TOF).

Results. Aptamer compositions examined exhibited a wide range of mean residence times in circulation (0.6–16 h) and significant variation in distribution levels among organs and tissues. Among the conjugates tested, *in vivo* properties of aptamers were altered most profoundly by conjugation with PEG groups. Complexation with a 20 kDa PEG polymer proved nearly as effective as a 40 kDa PEG polymer in preventing renal clearance of aptamers. Conjugation with 20 kDa PEG prolonged aptamer circulatory half-life, while reducing both the extent of aptamer distribution to the kidneys and the rate of urinary elimination. In contrast, the fully 2′-O-Me aptamer composition showed rapid clearance from circulation, and elimination with intact aptamer detectable in urine at 48 h post-administration.

Conclusions. We find that conjugation and chemical composition can alter fundamental aspects of aptamer residence in circulation and distribution to tissues. Though the primary effect of PEGylation was on aptamer clearance, the prolonged systemic exposure afforded by presence of the 20 kDa moiety appeared to facilitate distribution of aptamer to tissues, particularly those of highly perfused organs.

KEY WORDS: aptamer; biodistribution; conjugation; pharmacokinetics.

INTRODUCTION

Aptamers represent a promising class of therapeutic agents currently in preclinical and clinical development. Like biologicals such as peptides or monoclonal antibodies, aptamers are capable of binding specifically to molecular targets and, through binding, to inhibit target function. Created by an entirely *in vitro* selection process (SELEX) from libraries of random sequence oligonucleotides, aptamers have been generated against numerous proteins of therapeutic interest, including growth factors, enzymes, immunoglobulins, and receptors (1,2). A typical aptamer is 10–15 kDa in size (i.e., 30–45 nucleotides), binds its target with sub-nanomolar affinity, and discriminates among closely related targets (e.g., will typically not bind other proteins from the same gene family) (3–10). Aptamers have a number of attractive characteristics for use as therapeutics. In addition to high target affinity and specificity, aptamers have shown little or no toxicity or immunogenicity in standard assays (11). Several therapeutic aptamers have been optimized and advanced through varying stages of preclinical development, including pharmacokinetic analysis, characterization of biological efficacy in cellular and animal disease models, and preliminary safety pharmacology assessment (5,12,13). Several aptamers are now nearing, or have reached, the clinical development stage. Macugen, an angiogenesis inhibitor that targets vascular endothelial growth factor (VEGF), has advanced through clinical trials for age-related macular degeneration (AMD), a leading cause of blindness (14,15).

It is important for all oligonucleotide-based therapeutics, including aptamers, that their pharmacokinetic properties be tailored to match the desired pharmaceutical application. While aptamers directed against extracellular targets do not have to solve the problem of intracellular delivery (as do antisense and RNAi-based therapeutics), they must be capable of distributing to target organs and tissues and persist in the body unmodified for a period consistent with the desired dosing regimen. Earlier work on nucleic acid-based therapeutics has shown that while unmodified oligonucleotides are degraded rapidly by nuclease digestion, protective modifications at the 2′-position of the sugar and use of inverted terminal cap structures dramatically improve drug stability *in vitro* and *in vivo* (16–19). Thus, starting pools of nucleic acids from which aptamers are selected are typically pre-stabilized by chemical modification, for example by incorporation of 2′-fluoropyrimidine (2′-F) substituted nucleotides, to enhance resistance of aptamers against nuclease attack. Aptamers incorporating 2′-*O*-methylpurine (2′-O-Me) substituted nucleotides have also been developed through post-SELEX modification steps or, more recently, by enabling synthesis of 2′-O-Me–containing random sequence libraries as an integral component of the SELEX process itself (20,21).

In addition to clearance by nucleases, oligonucleotide therapeutics are subject to renal elimination. As such, a typical short, nuclease-resistant oligonucleotide administered intravenously exhibits an *in vivo* half-life of <10 min, unless filtration can be blocked by either facilitating rapid distribution out of the blood stream into tissues or by increasing the apparent molecular weight of the oligonucleotide above the effective size cut-off for the glomerulus. Conjugation of aptamers to a 40 kDa polyethylene glycol (PEG) polymer (PEGylation) can dramatically lengthen residence times of aptamers in circulation while marginally impacting the ability to bind to protein targets (5), thereby decreasing dosing frequency and enhancing effectiveness against vascular targets. Though previous work in animals has examined the plasma pharmacokinetic properties of PEG-conjugated aptamers (5,12), relatively little is known concerning the capacity of either unconjugated or PEGylated aptamers to escape the vasculature and distribute to organs and tissues *in vivo*. Knowledge concerning extravasation and in particular, the

[1] Archemix Corp., 1 Hampshire Street, Cambridge, Massachusetts 02139, USA.

[2] Address all correspondence to this author. (e-mail: mccauley@archemix.com)

0724-8741/04/1200-2234/0 © 2004 Springer Science+Business Media, Inc.

potential of aptamers or their modified forms to access diseased tissues (for example, sites of inflammation, or the interior of tumors) is expected to better define the spectrum of therapeutic opportunities for aptamer intervention, and to guide the informed choice of new targets for aptamer development.

A large body of literature documents the pharmacokinetic and biodistribution properties of phosphorothioate-containing antisense oligonucleotides, which clear rapidly from circulation, and distribute into tissues where elimination occurs slowly as a result of metabolic degradation (22–28). In contrast to antisense oligonucleotides, however, aptamers are in general longer (30–40 vs. 10–20 nucleotides), possess different types of chemical modifications (sugar, e.g., 2′-F, 2′-O-Me, 2′-NH_2, vs. backbone modifications), and assume complex tertiary structures that are, in many respects, more similar to the three-dimensional forms of globular proteins than to nucleic acids. Given these considerable differences, the *in vivo* disposition of aptamers is not readily predictable from antisense results. Earlier studies involving antisense oligonucleotides have explored the effects of various conjugation chemistries on pharmacokinetics and biodistribution, with the ultimate goal of increasing delivery of antisense molecules to their sites of action inside cells or within certain tissue types *in vivo* (29–33). For example, conjugation with cholesterol has been reported to increase the circulation half-life of antisense oligonucleotides, most likely through association with plasma lipoproteins, and to promote hepatic uptake (34). More recently, delivery peptides apparently able to carry large polar macromolecules, including oligonucleotides, across cellular membranes have also been explored as a means to augment *in vivo* the range for application of antisense and other therapeutics. Examples of these conjugates include a 13-amino acid fragment (Tat) of the HIV Tat protein (35), a 16-amino acid sequence derived from the third helix of the Drosophila antennapedia (Ant) homeotic protein (36), and short, positively charged cell-permeating peptides composed of polyarginine (Arg_7) (37,38).

In the current work, we examine the effects of conjugation of small molecule, peptide, and polymer terminal groups on the pharmacokinetics and biodistribution of stabilized aptamer compositions *in vivo*. Levels of aptamer conjugates in biologic samples are quantified radiometrically and by a hybridization-based dual probe capture assay with enzyme-linked fluorescent readout. We find that conjugation and chemical composition can alter fundamental aspects of aptamer residence in circulation and distribution to tissues. A mixed composition aptamer containing both 2′-F and 2′-O-Me stabilizing modifications persisted significantly longer in the blood stream than did a fully 2′-O-methylated composition. Furthermore, complexation with a 20 kDa PEG polymer proved nearly as effective as a 40 kDa PEG polymer in preventing aptamer elimination. Though the primary effect of PEGylation was on aptamer clearance, the prolonged systemic exposure afforded by presence of the 20 kDa moiety appeared to facilitate distribution of aptamer to tissues, particularly those of highly perfused organs.

MATERIALS AND METHODS

Aptamer Synthesis

The nucleotide sequence and predicted secondary structure of the parent oligonucleotide ARC83 are shown in Fig. 1.

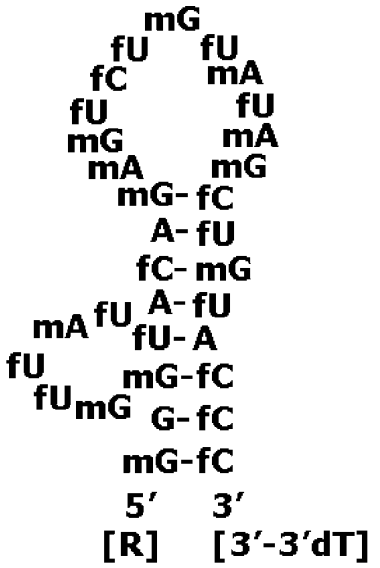

Fig. 1. Nucleotide sequence, composition, and secondary structure of aptamer ARC83. Conjugates (R = 40 kDa PEG, 20 kDa PEG, cholesterol, Tat, Ant, or Arg_7 peptides) were added at the 5′-terminus as described in "Materials and Methods." An inverted 3′-3′ dT structure caps the 3′-terminus. ARC83 is an inactive variant of an aptamer directed against TGFβ-2 (39) and was generated by scrambling the positions of stabilizing 2′-F and 2′-O-Me substitutions. Positions of 2′-O-Me substitution are denoted by lowercase m, while positions of 2′-F substitutions are denoted by lowercase f.

ARC83 is a 32-mer derived from a previously described aptamer specific for TGFβ-2 (37). Syntheses of ARC83 and its fully 2′-O-Me modified variant, ARC159, were performed using standard solid-phase phosphoramidite chemistry, followed by ion-exchange high-pressure liquid chromatography (HPLC) or polyacrylamide gel electrophoresis (PAGE) purification. All oligonucleotide syntheses were performed in-house, except for ARC83 (Dharmacon, Inc., Lafayette, CO, USA).

Synthesis of Aptamer Conjugates

ARC83 was conjugated to one of several different functional moieties to generate the following conjugates: 20 kDa PEG (ARC120); 40 kDa PEG (ARC122); HIV Tat peptide (ARC156); antennapedia (Ant)-derived peptide (ARC157); or poly-arginine (Arg7) (ARC158). The various modifications to ARC83 were made post-synthetically via amine-reactive chemistries. For the PEG conjugates, ARC83 was dissolved to 1 mM in 100 mM sodium carbonate buffer, pH 8.5, and was reacted for 1 h with a 2.5 molar excess of mPEG-SPA (mPEG-succinimidyl propionate; MW 20 kDa, Nektar Therapeutics, Birmingham, AL, USA) or mPEG2-NHS ester (MW 40 kDa) (Shearwater Corp., Huntsville, AL, USA) in an equal volume of acetonitrile. The resulting products were then purified by reverse phase HPLC on a Transgenomic OligoPrep HC column with acetonitrile, 50 mM TEAA (Triethylammonium acetate) as an eluent.

The peptide conjugates were prepared by reacting pyridyldithio-activated aptamers with C-terminal cysteine containing peptides. For this procedure, ARC83 was dissolved to 2 mM in 100 mM sodium carbonate buffer, pH 8.5, and a 6-fold molar excess of *N*-succinimidyl 3-(2-pyridyldithio) pro-

pionate (SPDP; Pierce, Rockford, IL, USA) was added. After 90 min at room temperature, the reactive intermediate was recovered through precipitation with isopropanol, resuspended in PBS buffer pH 7.4, and reacted for 3 h at room temperature with 2 mM solutions of RKKRRQRRRPPQC (Tat), RQIKIWFQNRRMKWKKGGC (Ant), or RRRRRRRC (Arg_7) (Tufts University Core Facility, Boston, MA, USA) in an equal volume of formamide. Products were purified by electrophoresis on preparative 20% (w/v) polyacrylamide gels. Lastly, a 5′-cholesterol-modified oligonucleotide (ARC155) was prepared by standard automated solid-phase synthesis using a cholesteryl-TEG phosphoramidite (1-dimethoxytrityloxy-3-*O*-(*N*-cholesteryl-3-aminopropyl)-triethyleneglycol-glyceryl-2-*O*-(2-cyanoethyl)-(*N,N*-diisopropyl)-phosphoramidite, Glen Research, Sterling, VA, USA).

Aptamer conjugate composition was verified by polyacrylamide and capillary gel electrophoresis, HPLC, and/or matrix-assisted laser desorption ionization time of flight mass spectrometry (MALDI-TOF). Conjugates were formulated for dosing after precipitation and desalting using CentriSep filters (Princeton Separations Inc., Adelphia, NJ, USA). A list of aptamers used in this study, summarizing aptamer name, conjugation status, composition, and molecular weight is shown in Table I.

[^{3}H]-Labeling of Aptamers

ARC83 and ARC159 were tritiated at ViTrax, Inc. (Placentia, CA, USA) using a heat-catalyzed tritium exchange reaction (40). ARC83 and ARC159 reaction products were determined to have high radiochemical purity (>98%) and specific activities of 850 μCi/mg and 760 μCi/mg, respectively. As reported previously, tritium did not back-exchange from [^{3}H]-ARC83 or [^{3}H]-ARC159 at room temperature or 37°C and the radiolabel was considered to have a physical stability suitable for *in vivo* experimental conditions (40). Samples of the tritiated 20 kDa PEG conjugate (ARC120) and the Arg_7-oligonucleotide (ARC158) were prepared as described above on a small scale, using [^{3}H]-ARC83 as starting material, followed by PAGE purification.

Dosing Formulations

Aptamers for the pharmacokinetic study were dissolved in 1X phosphate-buffered saline (PBS) (137 mM NaCl, 2.7 mM KCl, 10 mM NaHPO4, 2 mM KH2PO4, pH 7.2) at a concentration of 1 mg/ml prior to administration. For the biodistribution experiments involving tritiated aptamers, dosing formulations were prepared in 1X PBS to a final concentration of 1 mg/mL, with specific activities of 25 μCi/mg (ARC83), 52 μCi/mg (ARC120), 37 μCi/mg (ARC158), and 37 μCi/mg (ARC159).

TABLE I. Key to Aptamers and Aptamer-Conjugates Used in This Study

Aptamer	Conjugation status	Composition	Molecular weight
ARC83	None	2′-F/2′-O-Me	10,925
ARC120	20 kDa PEG	2′-F/2′-O-Me	30,924
ARC122	40 kDa PEG	2′-F/2′-O-Me	50,924
ARC155	Cholesterol	2′-F/2′-O-Me	11,167
ARC156	Tat peptide	2′-F/2′-O-Me	12,889
ARC157	Ant peptide	2′-F/2′-O-Me	13,588
ARC158	Arg_7 peptide	2′-F/2′-O-Me	12,181
ARC159	None	2′-O-Me	11,837

Animals and Experimental Procedures

Pharmacokinetic and biodistribution studies were performed using 8–10 week-old male Sprague-Dawley rats (250–300 g, Charles River Laboratories, Wilmington, MA, USA). Rats were fed *ad libitum* with a standard laboratory diet and housed under controlled conditions (12-h light cycle, 20°C) prior to experimentation. For experiments in which urine was collected, animals were housed in metabolic cage units with free access to food and water. Prior to dosing, rats were divided into treatment groups and each received a single intravenous administration of aptamer at a dose of 1 mg/kg body weight. For some experiments, animals were fitted with femoral and jugular vein catheters (Hilltop Lab Animals, Scottsdale, PA, USA) and doses (at a volume of 1 ml/kg) were administered as a bolus injection into the femoral vein catheter. Immediately following intravenous administration, the dosing catheter was flushed with 0.5 ml of 0.9% saline. Blood samples were collected from replicate animals (n = 3) in each group at time points of –0.25 (pre-dose), 0.25, 1, 3, 12, and 48 h via the jugular vein catheter. At 48 h, all animals were euthanized and selected tissues were collected. For biodistribution studies involving tritiated aptamers, each animal received a single 1 mg/kg intravenous bolus dose of [^{3}H]-labeled aptamer per animal: ARC83, 6.6 μCi; ARC120, 13.9 μCi; ARC158, 9.6 μCi; ARC159, 9.7 μCi, respectively. At time points of 3, 12, and 24 h postdosing, subgroups of animals (n = 2 per time point) for each aptamer conjugate were euthanized and blood samples and selected tissues collected. Blood samples were centrifuged immediately for isolation of plasma as described below. For the animals to be euthanized at 24 h post-dosing, urine was collected over the following intervals: 0-3, 3-6, 6-12, and 12-24 h post-dosing (n = 2 animals per group). For radioactive biodistribution studies involving tritium, control animals (n = 1 rat per time point) were dosed in parallel with cold, that is, unlabeled, versions of the same aptamers or aptamer conjugates, and blood, tissue, and urine samples collected as above.

Biological Sample Collection and Processing

Blood samples (0.4 ml) collected from animals at specified time points were drawn into tubes containing sodium-EDTA-containing as an anticoagulant (1.8 ml vacutainers., BD Biosciences, San Jose, CA, USA). Blood samples were placed immediately on wet ice and then processed by centrifugation for 10 min at approximately 4°C to yield plasma. Plasma samples were stored at –80°C until analysis. In biodistribution studies involving nonradioactive aptamers, selected tissues (brain, heart, kidneys, liver, spleen, bone marrow from both femurs) were collected at 48 h. The brain, heart, kidneys, liver and spleen were rinsed with 0.9% saline and then blotted dry prior to weighing. Organs were homogenized in saline using a Polytron homogenizer to produce a

50% tissue homogenate [1:1 (w/w) tissue:saline]. Each bone marrow sample (from both femurs combined) was homogenized in saline to produce a 20% tissue homogenate [1:4 (w/w) tissue:saline]. All tissue homogenates were stored at −20°C prior to analysis. To determine biodistribution of [^{3}H]-labeled aptamers, selected tissues (liver, kidneys, lungs, heart, spleen, brain, bone marrow (both femurs), gastrointestinal tract, eyes, mediastinal lymph nodes) were harvested at 3, 12 and 24 h postadministration.

Hybridization-Based Dual-Capture Assay for Aptamer Quantitation

The primary analytical method used to measure the concentration of intact, nonradioactive aptamer in plasma and tissue homogenate samples was a hybridization-based dual-capture psuedo-ELISA. In this assay, a biotinylated capture probe (ARC179, 5′ ACTCTGTAATAACCCC-[spacer18]-biotin) was preimmobilized in the wells of a 96-well microplate at a binding solution concentration of 125 nM (×100 μl/well = 12.5 pmole/well) for 3 h. The plate wells were washed 5 times using a Biotek Elx405 plate washer with 1X Dulbecco's PBS. The plates were then blocked with 150 μl /well of a solution containing 1X PBS, 0.05% Tween-20, 0.025% yeast tRNA (Sigma-Aldrich, St. Louis, MO, USA). Plates were washed again, covered, and stored at 4°C until use. In separate tubes, the samples(s) were annealed in a buffer containing the FAM-labeled (5′-Fluorescein Phosphoramidite modifier, Glen Research, Sterling, VA, USA) detection probe (ARC180, 5′ FAM-[spacer18]-GGGTACAGCTATACAG, at 200 nM) at 90°C for 10 min, then quenched on ice. Standard control samples, and the pre-annealed plasma/tissue sample-detection probe solutions were then pipetted (typically 1:5–1:1000-fold dilutions of the sample were assayed) into the plate wells containing the immobilized biotin capture probe, and annealed at 45°C for 2.5 h. Plates were then washed again, and filled with 100 μl /well of a solution containing 1 μg/ml of anti-fluorescein monoclonal antibody conjugated to horse radish peroxidase (anti-FITC MAb-HRP, Molecular Probes, Eugene, OR, USA) in 1X PBS, and incubated for 1.3 h. Plates were washed again as above. Wells were then filled with 100 ul of a solution containing a fluorogenic HRP substrate (QuantaBlu, Pierce Chemical, Rockford, IL, USA), and incubated for 30–45 min protected from light. After incubation, 100 ul/well of a stop solution was added to quench the fluorescent precipitate-producing reaction. Plates were read immediately on a fluorescence microplate reader (Fusion, Packard Biosciences, Billerica, MA, USA) with fluorescence excitation at 335–350 nm and emission detected at 460 nm. Each well was read 10 times, with a 1 min interval between plate reads. The mean relative fluorescence value (RFU), standard deviation, and % CV for all reads of each plate were written to an electronic file for subsequent analysis.

Data files were imported into previously prepared MS Excel templates for preliminary analysis and formatting. Kaleidagraph was used to fit the RFU signal vs. concentration curves for duplicate or triplicate control standards included on each plate. Once a standard concentration curve was generated for a given sample plate, the plasma/tissue sample well signals were analyzed to determine the concentration of full-length aptamer present in each sample.

Measurement of Radioactivity

Each sample was prepared for analysis of total [^{3}H]- radioactivity in duplicate. Aliquots of known size of each urine, metabolic cage rinse, and plasma sample were mixed with 10 mL of Ultima Gold (Packard BioSciences Co., Meriden, CT, USA) liquid scintillation cocktail for direct analysis by liquid scintillation counting (LSC). All other samples (or aliquots of samples) were combusted prior to LSC analysis. Aliquots of samples analyzed by combustion were weighed into combustion boats and combusted in a Harvey Biologic Materials Oxidizer (Model OX500 or OX300, R. J. Harvey Instrument Co., Hillsdale, NJ, USA). Each aliquot was combusted for 4 min. The liberated $[^3H]_2O$ was trapped in 15 ml of Monophase S liquid scintillation cocktail (Packard Bioscience Co.). A solution of each radiolabeled aptamer was used as an oxidation standard. The LSC results for combusted samples were corrected for the efficiency of the oxidizer as determined on the day the specific samples were combusted.

Radioactivity was quantitated by LSC using a Beckman Model LS 6000TA or LS 6500 liquid scintillation spectrophotometer (Beckman Instruments Inc., Fullerton, CA, USA). Count data were automatically corrected for chemical quench, as determined using a ^{137}Cs external standard. All samples were counted for 10 min or until a 2-σ error of 1% was achieved. Analyses were considered acceptable if the duplicate dpm/g or dpm/mL values were within 10% of the mean value, provided the mean per aliquot analyzed was >100 dpm. The sensitivity of the radio-analytical procedures was estimated assuming that a minimum of 150 dpm (above a background of approximately 50 dpm) per aliquot assayed was required for quantitation. Approximate mean sample size, aliquot size, and dose were used in the calculations. The [^{3}H]-content of each sample was adjusted for total tissue weight and expressed as a percentage of the administered dose, or as the equivalent concentration of aptamer (μg equiv/ml or μg equiv/gram). In terms of concentration, actual quantitation limits ranged from 0.0013 μg/g to 0.26 μg/g. In terms of percent of dose, actual quantitation limits ranged from 0.00051% of dose to 0.025% of dose.

Pharmacokinetic Models and Parameters

An initial pharmacokinetic analysis of anti-TGFβ–2 aptamer in rats following intravenous bolus injection was carried out by Gilead Sciences, Inc. (39). Its observed pharmacokinetic profile appeared to be biphasic and described by a two-compartment model. In the present study, we also found the pharmacokinetic profile of the scrambled anti-TGFβ–2-derived aptamer (ARC83) to be well-described by a two-compartment model. It should be noted, however, that the behavior of the unconjugated, fully 2′-O-Me version of the aptamer (ARC159) showed a monophasic profile and could only be modeled by a one-compartment model or by non-compartmental analysis. The concentration vs. time data for all aptamer conjugates was imported into software package WinNonlin (Pharsight Corp., Mountainview, CA, USA) for analysis.

Detection of Intact Aptamers

The primary analytical method used to measure the concentration of intact, nonradioactive aptamers in biological samples (plasma, tissue, urine) was the hybridization-based dual-capture psuedo-ELISA described above. Additional bioanalytical methods used included capillary gel electrophoresis (CGE), and MALDI-TOF. For CGE analysis, samples spiked with 50 pmole of an oligonucleotide (T_{20}) internal standard were incubated in buffer (60 mM Tris-Cl, pH 8.0, 100 mM EDTA, 0.5% SDS) containing proteinase K at 500 μg/ml at 65°C for 4 h. Digests were extracted twice with phenol/chloroform, and then precipitated with ammonium acetate. CGE (Beckman P/ACE 5010) was performed at 25°C using 10% polyacrylamide gel-filled capillaries and an applied voltage of 20 kV. Elution of oligonucleotides was monitored using UV detection at 260 nm. Under these conditions, resolution of aptamers from chain-shortened metabolites could be achieved. MALDI-TOF analysis was performed using an ABI Voyager-DE PRO mass spectrometer in linear mode (Applied Biosystems, Foster City, CA, USA). Urine samples for mass spectrometry were purified on ZipTip C18 pipette tips (Millipore, Billerica, MA, USA).

RESULTS

We have defined plasma pharmacokinetic and tissue distribution properties of stabilized aptamer compositions and assessed the ability to alter both plasma half-life and biodistribution through use of small and high molecular weight polymer tags. Oligonucleotide ARC83 (Fig. 1) is an inactivated model aptamer containing 2′-F and 2′-O-Me modifications, as well as a 3′-inverted-dT cap for enhanced stability against nuclease attack, and a 5′-terminal amino modifier for subsequent conjugation reactions. Though identical in composition to a previously reported anti-TGF-β2 aptamer (39), ARC83 does not bind TGF-β2 due to scrambling of 2′-modifications at selected positions in the molecule (specifically the conversion of 2′-hydroxyls to O-methyl groups at nucleotides 2, 10, 12, and 29 and the reverse conversion of 2′-O-methyls to hydroxyls at nucleotides 7, 19, 21, and 23). With these modifications, the ability to form the appropriate tertiary structure required for ligand binding is lost while the base sequence (and presumably the secondary structure) of the active molecule is maintained. ARC159 is similarly a biologically inert variant of ARC83 which bears a 2′-O-methyl substitution at every nucleotide. By studying the pharmacokinetic and biodistribution properties of inactive aptamers, potentially confounding effects of target binding on *in vivo* characteristics can be avoided. Both ARC83 and ARC159 exhibit a high degree of resistance to plasma nucleases *in vitro*, as judged by denaturing PAGE following incubation of radiolabeled aptamers in the presence of 95% rat plasma (data not shown). The *in vitro* half-life of ARC83 is >24 h, while the fully 2′-O-methyl aptamer, ARC159, is almost entirely stable up to 96 h (Archemix Corp. unpublished data).

Development of a Hybridization-Based Assay for Determination of Aptamer Pharmacokinetics

To facilitate *in vivo* studies, we developed a hybridization-based dual probe capture assay with enzyme-linked fluorescent readout for monitoring the concentration of intact, undegraded aptamer in biologic samples (Fig. 2A). The assay relies upon a capture probe attached to a solid support (a 96-well plate bottom), and a FAM-labeled detection probe. When the aptamer-containing sample and probes are combined in the assay well, the pre-immobilized capture probe forms a hybrid with the 5′ end of the oligonucleotide (aptamer) to be detected and the pre-annealed detection probe forms a hybrid with the 3′ end. Following extensive washing to remove free probe molecules, an anti-FAM-HRP conjugate is combined to generate a fluorescent signal proportional to the concentration of retained probe-aptamer complex.

As shown in Fig. 2B, the lower limit of detection achievable with this assay is 50-100 pM (~0.8 ng/ml, based on aptamer weight without conjugation), while the upper limit of detection is ~25 nM (264 ng/ml, based on aptamer weight without conjugation). The resulting dynamic range is ≥250-fold. To ensure that sample concentrations were within the dynamic range for the assay, a range of dilutions of each sample was analyzed. For time points shortly after the initial dosing, larger dilution factors (~1:100–1:1000) were used, whereas for later time points, dilution factors of 1:5–1:10 were suitable for accurate detection and quantitation. In general, several sample dilution points were within the linear dynamic range of the assay, and thus provided a measure of the precision of the assay. The data sets resulting from the dual-capture ELISA assay constitute concentration vs. time data for the aptamer conjugates. This data was then fitted, analyzed, and compared against data generated by pharmacokinetic models of the system under investigation, in order to extract parameters such as the characteristic half-life of the aptamer in the blood, the maximum concentration observed, the total integrated dose administered, overall clearance rate, and volume of distribution.

Pharmacokinetic Profiles of Aptamer Conjugates in Plasma

Using the hybridization-based assay, we determined the concentration of aptamer-derived conjugates as a function of time following intravenous bolus administration to rats. Aptamer conjugates were formed by attachment of activated tags to a synthetically incorporated 5′-amino group of ARC83 as described in "Materials and Methods." Aptamers and aptamer conjugates used in this study are listed in Table I. Conjugates tested included 20 kDa and 40 kDa PEGs, cholesterol, and a set of peptides previously reported to facilitate extravasation and/or cellular uptake of conjugated molecules (including an Ant-derived peptide, a Tat-derived peptide, and Arg_7) (29–33). As shown in the standard curves for different aptamer conjugates in Fig. 2B, the limit of detection for the assay is relatively unaltered as a result of aptamer conjugation. The presence of plasma or tissue homogenates decreased the sensitivity of the assay under typical dilution conditions to a lower limit of detection of approximately 100–200 pM (data not shown).

Figure 3 depicts the *in vivo* plasma pharmacokinetic profiles in rat of unconjugated and conjugated aptamers measured at intervals over 48 h. Primary and secondary pharmacokinetic parameters extracted from analysis of the concentration vs. time data in the context of a biphasic, two-compartment model are presented in Table II. Reported concentrations for both plasma and tissue analysis refer only

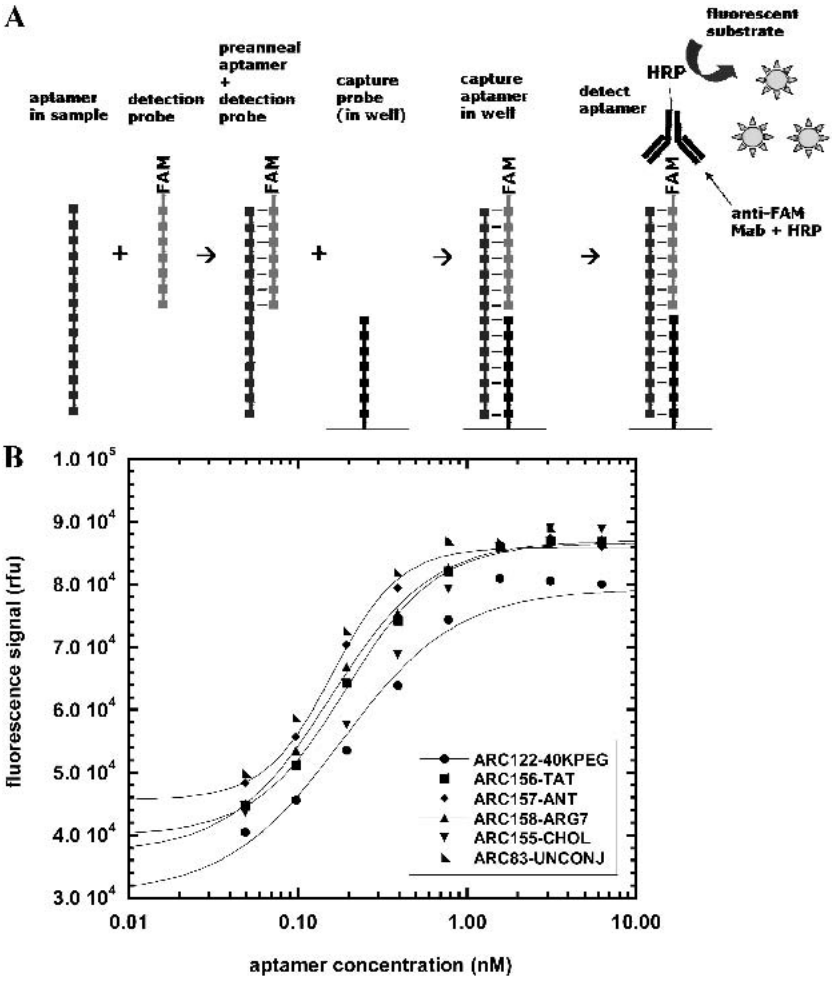

Fig. 2. (A) Schematic of hybridization-based, dual-capture assay used for quantitative analysis of full-length aptamers in biologic samples. (B) Typical standard curve data for the assay in rat plasma, performed as described in "Materials and Methods," showing the upper and lower limits of detection, displacement, and dynamic range.

to full-length aptamer sequence, and do not include the molecular weight of any associated conjugations, such as PEGylation. The unconjugated 2′-F/2′-O-Me-modified aptamer (ARC83) was reasonably long-lived, displaying a $t_{1/2}$ (β) of nearly 5 h and mean residence time of close to 1.7 h The relatively large volume of distribution (approximately 460 mL/kg) of ARC83 suggested that even in the absence of conjugation, the aptamer does distribute to tissues to some degree (Fig. 3A and Table II). As expected, the 40 kDa PEG-conjugate (ARC122) showed a substantially longer half-life in circulation ($t_{1/2}$ (β) of nearly 12 h) and a significantly reduced volume of distribution (144 ml/kg). Notably, the mean residence time for the 40 kDa PEG-conjugate (nearly 16 h) was approximately 10-fold greater than that for unconjugated aptamer. Consistent with these results, the 20 kDa PEG-conjugate (ARC120) exhibited intermediate values for half-life in circulation ($t_{1/2}$ (β) of approximately 7 h) and mean residence time (close to 8 h) relative to both unconjugated aptamer and to the 40 kDa PEG conjugate (Fig. 3A and Table II). While PEGylation slowed clearance of the aptamer from the circulatory volume, neither 20 kDa nor 40 kDa PEG conjugation obviously enhanced the apparent distribution of the aptamer into extravascular spaces as judged by their calculated volumes of distribution (Vss, Table II). Notably, the 20 kDa PEG conjugate (ARC120) showed a significantly higher AUC value relative to the 40 kDa PEG conjugate (ARC122).

The fully 2′-O-Me composition aptamer (ARC159) displayed much more rapid elimination from plasma compared to unconjugated aptamer. Indeed, ARC159 showed the shortest mean residence time in the blood stream (roughly 30 min) of any of the aptamers tested (Fig. 3A and Table II). The pharmacokinetic profile of ARC159 was also distinctive in that it displayed a monophasic pharmacokinetic profile best described by one-compartment or noncompartmental models. In contrast to unconjugated aptamer, conjugates bearing cholesterol (ARC155) and Tat (ARC156) could not be detected in plasma by 12 h using the hybridization assay (Fig. 3B), suggesting an increase in their rates of clearance. The other cell permeating peptide-conjugates tested, ARC157 (Ant) and ARC158 (Arg_7) did not differ markedly from unconjugated aptamer (ARC83) in terms of their pharmacokinetic parameters (Fig. 3B and Table II).

In a separate study, we also quantitated levels of radiolabeled aptamers or conjugates in rats following intravenous bolus administration. Plasma concentrations of [^{3}H]-aptamer equivalents for ARC83, ARC120, ARC158, and ARC159

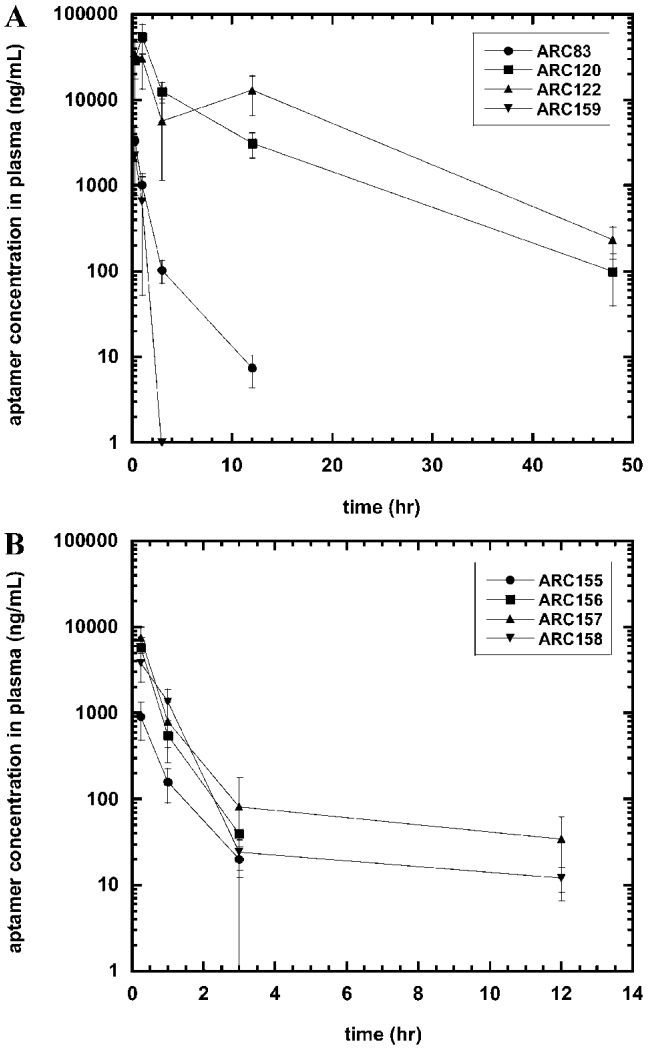

Fig. 3. Plasma pharmacokinetic profiles of aptamer conjugates determined via the dual-capture hybridization assay. Concentration of aptamer is shown as a function of time following a single bolus, intravenous injection in Sprague-Dawley rats. Concentrations are given in nanograms of oligonucleotide, not conjugated aptamer. (A) ARC83 (unconjugated); ARC120 (20 kDa PEG); ARC122 (40 kDa PEG); ARC159 (fully 2′-O-Me composition). (B) ARC155 (cholesterol); ARC156 (Tat peptide); ARC157 (Ant peptide); ARC158 (Arg_7 peptide).

over time showed the same trends seen for nonradioactively labeled aptamers measured using the hybridization-based assay (data not shown). The relative abundance of full-length aptamer conjugates at all time points showed the following relation: [ARC120, 20 kDa PEG] > [ARC83, unconjugated] > [ARC158, Arg_7] > [ARC159, 2′-O-Me], with the concentrations of all aptamers decreasing from 3 to 24 h The concentration of [^{3}H]-ARC83 (unconjugated) and [^{3}H]-ARC158 (Arg_7) equivalents were in the range of 450 to 700 ng/mL, whereas the concentration of [^{3}H]-ARC159 (2′-O-Me) equivalents ranged from approximately 200 to 400 ng/mL by 24 h after dosing. Notably, for ARC120 (20 kDa PEG), [^{3}H]-aptamer equivalent concentrations at 3 h post-dosing were approximately an order of magnitude greater than for the other aptamers; the concentration of ARC120 then decreased to a level similar to that of the other aptamers (data not shown).

In parallel, plasma concentrations of ARC83, ARC120, ARC158, and ARC159 were determined by dual-capture ELISA in animals dosed with cold aptamers. These values were 100–350 ng/ml (ARC83), 250–2000 ng/ml (ARC120), 20–50 ng/ml (ARC158), and 15–50 ng/ml (ARC159). Taking the ratio of aptamer concentrations measured using the dual-hybridization ELISA assay to those obtained using LSC gives an estimate of the fraction of full-length aptamer present in the plasma at each time point. The full-length fractions derived using this method ranged from 22-42% at 3 h for all aptamer conjugates tested.

Analysis of Aptamer Distribution to Tissues

Aptamer concentrations in terminal tissue samples harvested 48 h post-administration were quantified by dual capture ELISA. Significant levels of several aptamer species, most notably ARC159 were detected in kidney, and to lesser extent, in liver and spleen (Fig. 4). The high levels of ARC159 found in these organs at 48 h relative to other aptamers could reflect the extremely high degree of intrinsic stability against nuclease attack *in vivo* conferred by saturating 2′-O-Me modification. The kidneys also represented the major target for distribution of the Tat (ARC156) and Ant (ARC157) peptide conjugates (Fig. 4).

Biodistribution of Radiolabeled Aptamers

Distribution of tritiated aptamers ARC83 (unconjugated), ARC120 (20 kDa PEG), ARC158 (Arg_7), and ARC159 (fully 2′-O-Me) to ten different organs or tissues (liver, kidney, lungs, heart, spleen, brain, bone marrow, gastrointestinal tract, eyes, and mediastinal lymph nodes) was determined *in vivo* over time in rats receiving a single intravenous bolus administration of each aptamer. Tissues plasma, and urine were collected at intervals and analyzed for total radioactivity [^{3}H] by oxidation and subsequent liquid scintillation analysis.

Among organs examined, greatest uptake of [^{3}H]-aptamer equivalents (normalized with respect to the administered dose) was found in the kidney and liver (Fig. 5). The gastrointestinal tract also showed measurable levels of all aptamers. From a qualitative stand point, aptamer biodistribution profiles established by 3 h were largely maintained over the 24 h duration of the experiment. While the observed tissue distribution profiles of [^{3}H]-aptamers were generally similar among the aptamers tested, there were a few notable differences. For [^{3}H]-ARC120 (20 kDa PEG), uptake by the kidneys accounted for <5% of the administered dose at all sampling times, whereas for ARC159 (fully 2′-O-Me), uptake by the kidneys accounted for >20% of the administered dose. Indeed, levels of ARC120 in the kidney were significantly below levels of all of the other aptamers at all time points examined, consistent with the ability of 20 kDa PEG conjugation to reduce renal clearance and thereby prolong aptamer residence in circulation. Conversely, except for the kidneys, dose-normalized levels of [^{3}H]-ARC120 equivalents in the liver were higher than for the other aptamers (Fig. 5). Overall, the subset of organs/tissues assayed here accounted for uptake of ~35–70% of the administered dose.

In Fig. 6, distribution of [^{3}H]-aptamer equivalents is

TABLE II. Pharmacokinetic Parameters of Aptamer Conjugates

Conjugate	AUC (ng · h/ml)	Cmax (ng/ml)	A (ng/ml)	B (ng/ml)	$t_{1/2}$ (α) (h)	$t_{1/2}$ (β) (h)	MRT (h)	CL (ml · kg^{-1} · min^{-1})	Vss (ml/kg)
None ARC83	3573.39 ± 262	5009.40 ± 381	4926.20 ± 360	83.20 ± 73	0.42 ± 0.04	4.88 ± 3.47	1.66 ± 0.91	4.66 ± 0.34	464.28 ± 232.08
20 kDa PEG ARC120	146343.66 ± 3280	31323.00 ± 522	21711.83 ± 1153	9611.79 ± 1149	1.47 ± 0.11	7.23 ± 0.57	7.81 ± 0.42	0.11 ± 0.003	53.34 ± 2.21
40 kDa PEG ARC122	110009.41 ± 70996	14223.19 ± 10348	8106.47 ± 9904	6116.72 ± 5603	0.60 ± 1.63	11.68 ± 11.77	15.84 ± 15.09	0.15 ± 0.09	144.97 ± 94.32
Cholesterol ARC155	778.58 ± 24	1711.05 ± 85	1649.00 ± 78	62.06 ± 26	0.26 ± 0.02	1.79 ± 0.53	0.83 ± 0.14	21.40 ± 0.67	1067.20 ± 163.54
Tat ARC156	4222.22 ± 381	12885.00 ± 1670	12855.40 ± 1661	30.40 ± 54	0.22 ± 0.02	4.93 ± 9.53	0.66 ± 0.96	3.95 ± 0.36	156.38 ± 219.07
Ant ARC157	6211.96 ± 53	16229.75 ± 131	16120.14 ± 130	109.60 ± 6	0.22 ± 0.002	6.87 ± 0.45	1.99 ± 0.16	2.68 ± 0.02	320.94 ± 23.09
Arg_7 ARC158	3983.08 ± 715	5634.51 ± 784	5623.24 ± 777	11.27 ± 40	0.46 ± 0.07	16.34 ± 60.77	2.19 ± 7.88	4.18 ± 0.75	549.65 ± 1907.22
2′-O-Me ARC159	2013.84 ± 180	3614.53 ± 464.56	3614.53 ± 464.56	—	0.39 ± 0.05	—	0.56 ± 0.07	8.28 ± 0.74	276.66 ± 35.59

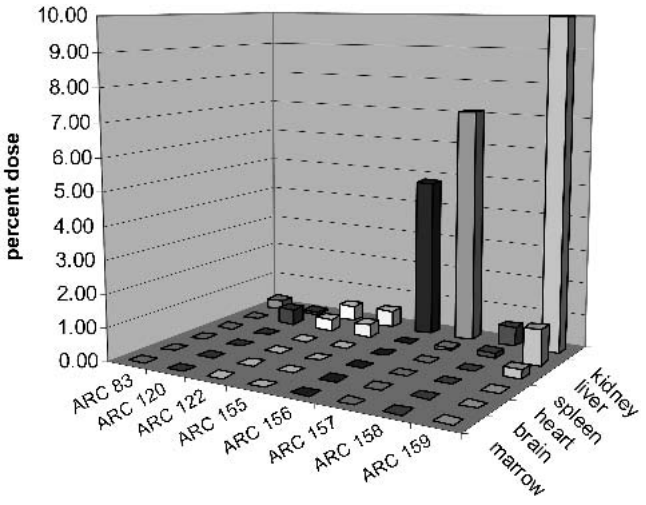

Fig. 4. Biodistribution of aptamers determined via dual-capture hybridization assay. Dose-normalized levels of aptamers tissue homogenates are shown following a single bolus, intravenous injection in Sprague-Dawley rats. Homogenates were prepared from the indicated organs or tissues at 48 h postdosing.

shown with data correction for organ or tissue weight. In general, greatest mass-normalized concentrations of [^{3}H]-aptamer equivalents were seen in highly perfused organs such as kidney, liver, spleen, heart, and lungs. Interestingly, comparatively high levels of each of the four aptamers or aptamer conjugates were also detected in the mediastinal lymph nodes (Fig. 6). For animals dosed with [^{3}H]-ARC83 (unconjugated), [^{3}H]-ARC158 (Arg_7), and [^{3}H]-ARC159 (2′-O-Me), the major organ of distribution was the kidney, with ARC159 showing the highest concentration by 3 h post-administration. Levels of [^{3}H]-aptamer equivalents in the kidneys showed the following relation: [^{3}H]-ARC159 (2′-O-Me) > [^{3}H]-ARC158 (Arg_7) > ARC83 (unconjugated) > ARC120 (20 kDa PEG). Interestingly, among all organs and tissues examined, highest mass-normalized concentrations of 20 kDa PEGylated aptamer (ARC120) were measured in the mediastinal lymph nodes rather than the kidneys (Fig. 6B).

Urinary Elimination of Aptamers

Despite some variability between the two replicate animals dosed for each aptamer, total urinary output during the 24 h following administration was generally similar. Interestingly however, the timing and extent of urinary elimination differed among the aptamers. Total urinary elimination hovered between 20-30% of the administered dose for [^{3}H]-ARC120 (20 kDa PEG) and [^{3}H]-ARC158 (Arg_7), 30–35% of the administered dose for [^{3}H]-ARC83 (unconjugated), and more than 40% of the administered dose for [^{3}H]-ARC159 (2′-O-Me) (Fig. 7). Consistent with these findings, intact [^{3}H]-ARC159 was most abundant in kidney, with aptamers showing the relation: [^{3}H]-ARC159 (2′-O-Me) > [^{3}H]-ARC158 (Arg_7) > [^{3}H]-ARC83 (unconjugated) > [^{3}H]-ARC120 (20 kDa PEG) (Fig. 5). Analysis of urine samples using capillary gel electrophoresis and MALDI-TOF detected presence of full-length ARC159 (2′-O-Me), but not other aptamers at 3 h (Fig. 8 and data not shown).

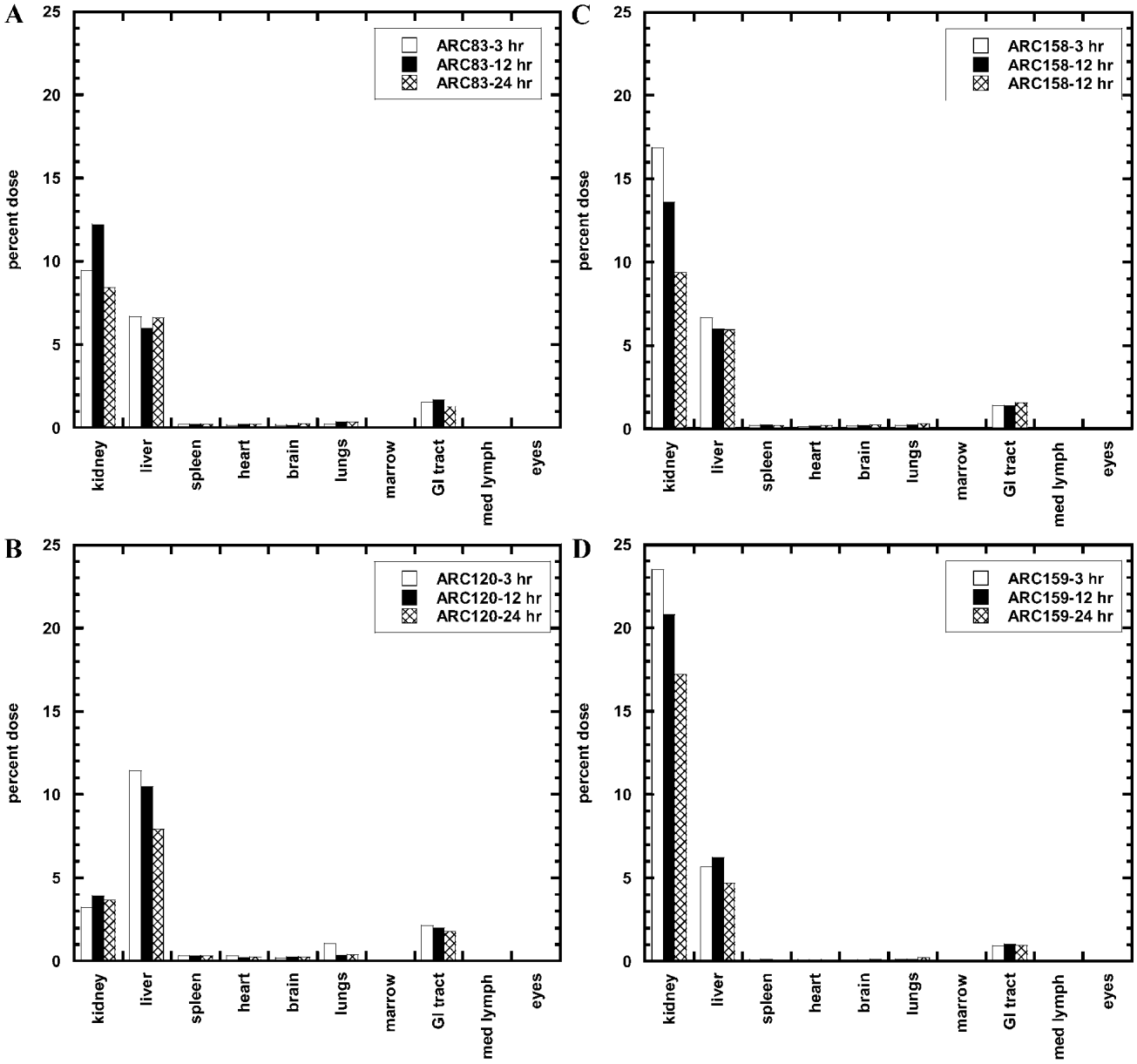

Fig. 5. Biodistribution of [^{3}H]-labeled aptamer conjugates. Dose-normalized levels of [^{3}H]-aptamer equivalents in the indicated organs or tissues were determined by combustion followed by LSC as described in "Materials and Methods." Organs or tissues were harvested at 3, 12, or 24 h postadministration of aptamers to Sprague-Dawley rats as a single bolus intravenous dose. (A) ARC83 (unconjugated), (B) ARC120 (20 kDa PEG), (C) ARC 158 (Arg_7 peptide), (D) ARC159 (fully 2′-O-Me composition).

DISCUSSION

Determination of aptamer plasma pharmacokinetics and biodistribution reported here has helped to define the utility of various aptamer conjugates and compositions for future therapeutic applications. A significant finding of the current study is the "tunability" of aptamer pharmacokinetics that can be achieved through conjugation and altered chemical composition. Unconjugated test aptamer ARC83 is typical of current generation aptamers in that it incorporates both 2′-F and 2′-O-Me stabilizing chemistries, and as a result, exhibits a high degree of nuclease stability *in vitro* and *in vivo*. Notably, ARC83 showed a relatively long *in vivo* half-life in the blood stream, even in the absence of any conjugation, and a volume of distribution consistent with limited extravascular access. Interestingly however, near complete elimination of ARC83 from circulation was observed by 48 h. Pharmacokinetic tunability is attractive for a number of treatment options (e.g., in antineoplastic or acute care settings where rapid drug clearance or turn-off may be desired). On the other hand, residence times of aptamers in circulation were prolonged by conjugation with high molecular weight polymers, with modulating effects produced by both 20 kDa and 40 kDa PEG species. In contrast to ARC83, significant levels of 20 kDa PEGylated aptamer (ARC120) persisted in plasma at 48 h, and its volume of distribution was smaller than that estimated for ARC83, suggesting preferential localization of ARC120 to the intravascular space and to highly perfused organs.

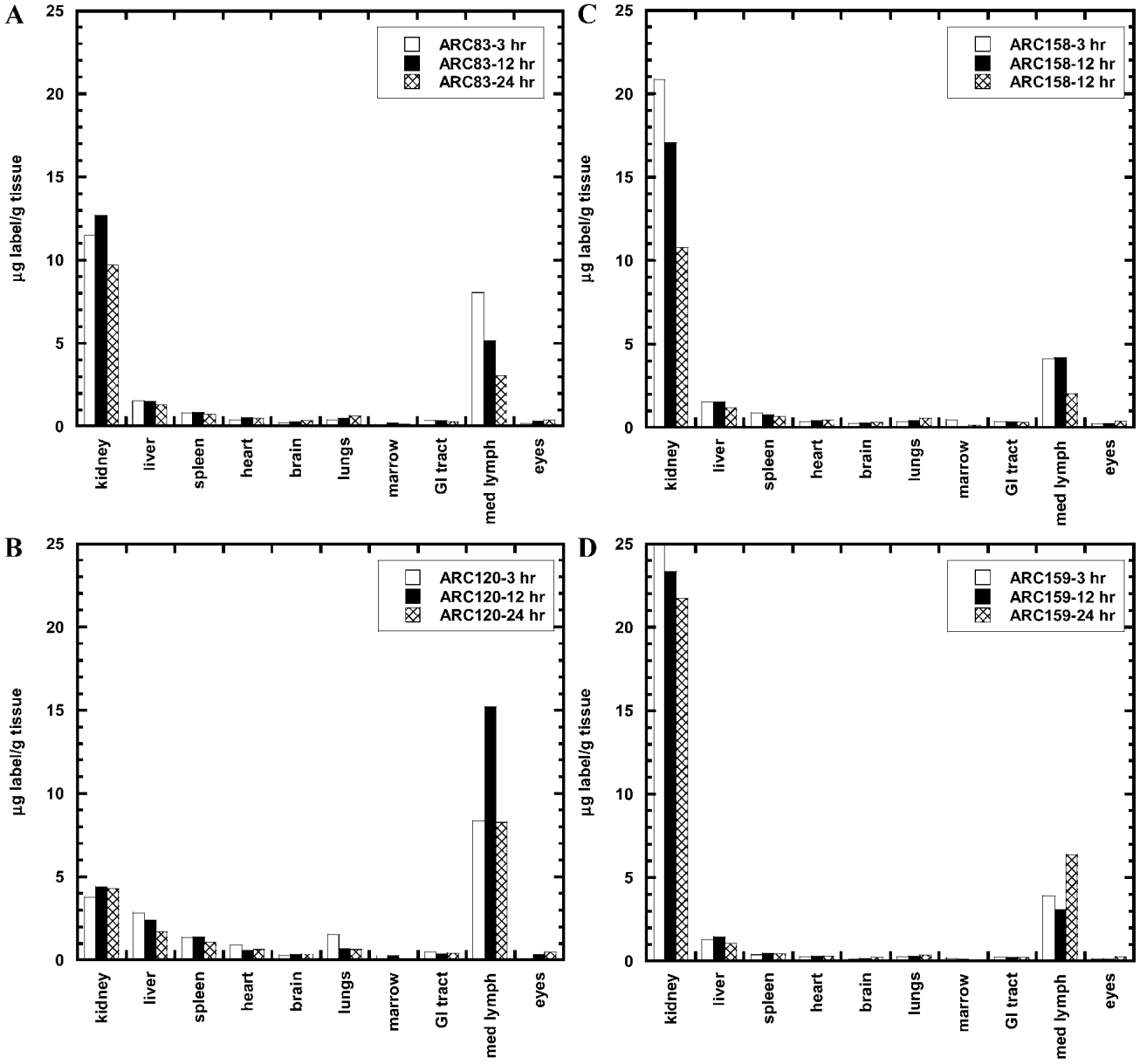

Fig. 6. Biodistribution of [^{3}H]-labeled aptamer conjugates. Mass-normalized levels of [^{3}H]-aptamer equivalents in the indicated organs or tissues were determined as described in Fig. 5 and expressed as micrograms of [^{3}H] label per gram of tissue. (A) ARC83 (unconjugated), (B) ARC120 (20 kDa PEG), (C) ARC 158 (Arg_7 peptide), (D) ARC159 (fully 2-O-Me composition).

Overall, effects on aptamer pharmacokinetics and tissue distribution produced by low molecular weight tags, including cholesterol and cell-permeating peptides were less pronounced than those produced as a result of PEGylation or altered chemical composition. The cholesterol conjugate (ARC155) showed more rapid plasma clearance relative to unconjugated aptamer, and a large volume of distribution suggestive of some degree of aptamer extravasation. However, this result appears to be somewhat at odds with published data demonstrating the capacity of a cholesterol tag to significantly prolong the plasma half-life of an antisense oligonucleotide (34). Potential explanations for results seen here are that cholesterol-mediated associations with plasma lipoproteins, postulated to occur in the case of the antisense conjugate, were precluded in the particular context of the ARC155 folded structure, and/or reflect some aspect of the lipophilic nature of the cholesterol group. Like cholesterol, presence of a Tat peptide tag appeared to promote clearance of aptamer from the blood stream, with comparatively high levels of conjugate appearing in the kidneys at 48 h. Other peptides (Ant, Arg_7) that have been reported to mediate passage of macromolecules across cellular membranes *in vitro* and translocation through vessel walls in *ex vivo* models (41), did not obviously promote aptamer clearance from circulation. However like Tat, the Ant conjugate was seen to accumulate significantly in the kidneys relative to other aptamers. It remains a formal possibility that unfavorable presentation of the Ant and Arg_7 peptide tags in the context of three dimensionally folded aptamers *in vivo* impaired their abilities to influence aptamer transport properties.

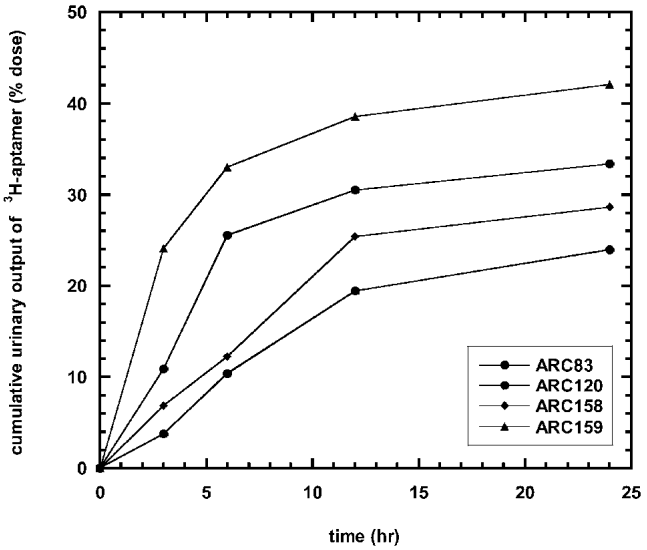

Fig. 7. Urinary elimination of [^{3}H]-labeled aptamer conjugates. Urine was collected at intervals from Sprague-Dawley rats receiving a single bolus intravenous dose of the indicated aptamers as described in "Materials and Methods." Dose-normalized [^{3}H]-aptamer equivalents in urine samples were measured by LSC. ARC83 (unconjugated); ARC120 (20 kDa PEG); ARC 158 (Arg_7 peptide); ARC159 (fully 2′-O-Me composition).

Prior to this work, relatively little was known concerning the pharmacokinetics and biodistribution of oligonucleotides with a 2′-O-Me chemical composition (42). For several reasons, incorporation of 2′-O-Me substitutions is a particularly attractive means to stabilize aptamers against nuclease attack. A primary attribute is safety: 2′-O-methylation is known as a naturally occurring and abundant chemical modification in eukaryotic ribosomal and cellular RNAs. Human rRNAs are estimated to contain roughly one hundred 2′-O-methylated sugars per ribosome (43). Thus, aptamer compositions incorporating 2′-O-Me substitutions are expected to be non-toxic. In support of this view, *in vitro* and *in vivo* studies indicate that 2′-O-Me nucleotides are not readily polymerized by human DNA polymerases (α or γ), or by human DNA primase, and thus, pose a low risk for incorporation into genomic DNA (44,45). Second, from a cost of goods perspective, pricing per gram for synthesis of 2′-O-Me containing oligonucleotides is less than that for both 2′-F and 2′-OH containing RNAs.

Compared to mixed 2′F/2′-O-Me composition aptamer ARC83, the fully 2′-O-Me modified aptamer (ARC159) displayed very rapid loss from plasma and distribution into tissues, with the primary target organ being the kidney. Nonspecific protein-binding interactions are known to play an important role in the characteristic, rapid loss of phosphorothioate-containing antisense oligonucleotide from circulation and distribution to tissues (22–28). It is not yet known whether the hydrophobic nature of ARC159 may render the oligonucleotide more prone to nonspecific associations with plasma or cellular components although previous studies with related 2′-O-alkyl modifications (e.g., 2′- methoxy-O-ethyl, (46) suggest a modest effect is likely. Due most likely to the extreme robustness of ARC159 toward nuclease digestion, levels of full-length ARC159 above background could be detected in several tissues (kidney, liver, spleen) even at 48 h after dosing. Consistent with its plasma clearance profile and distribution to the kidney, ARC159 was eliminated rapidly via the urine, where intact aptamer could be detected by capillary gel electrophoresis and MALDI-TOF analysis.

When expressed as percent of administered dose, all aptamers or conjugates examined showed significant levels of distribution to kidney, liver, and gastrointestinal tract. None of the aptamer conjugates or compositions showed a propensity to traverse the blood/brain barrier. When corrected for organ/tissue weight, highest mass-normalized concentrations of aptamers were seen in highly perfused organs (kidneys, liver, spleen, heart, lungs) and mediastinal lymph nodes. Since aptamers are bioavailable (up to 80%) following subcutaneous injection (13), they are expected to have access to targets in the lymphatic system through this route of administration. Ready access to the lymphatics via intravenous dosing may also of interest from the standpoint of developing aptamer therapeutics for infectious disease indications such as HIV/AIDS.

Consistent with its enhanced plasma pharmacokinetics, concentrations of 20 kDa PEGylated aptamer (ARC120) detected in highly perfused organs were higher than for the other aptamers. As a general trend, aptamer concentrations measured in the kidneys decreased with time, again with notable exception of ARC120, where concentrations remained roughly constant over time. Conversely, in liver concentrations of all aptamers remained roughly constant, except for ARC120, whose levels decreased with time. These differences may be understood in terms of the extended plasma half-life of the 20 kDa PEG conjugate and its increased uptake in highly perfused organs. Though the main effect of chemical conjugation with 20 kDa PEG was to retard renal elimination of aptamer, the comparatively high concentrations of 20 kDa PEG conjugate measured in well-perfused organs, relative to other aptamers or conjugates, suggests that PEGylation may also promote aptamer distribution to tissues. It is attractive to speculate that prolonged residence in the blood stream may increase exposure of conjugated aptamer to tissues, leading to enhanced uptake that is most pronounced in the case of highly perfused organs. Presence of aptamer in residual blood may contribute to, but is unlikely to account entirely for, increased levels of the 20 kDa aptamer conjugate seen in perfused organs. That enhanced distribution of PEGylated aptamer to perfused organs actually represents extravasation is suggested by results of recent autoradiography experiments in which [^{3}H] signal is evident inside cells of both liver and kidney in mice dosed with tritiated ARC120 (20 kDa PEG conjugate) (manuscript in preparation). Earlier work on aptamer therapeutics has focused primarily on development of aptamers complexed with higher molecular weight (40 kDa) PEG species to avoid renal clearance (5,12,13). The present study suggests that complexation with a smaller, for example, 20 kDa PEG polymer, may sufficiently protect aptamer-based drugs from elimination for many therapeutic indications, while providing collateral benefits in terms of ease of synthesis and reduced cost of goods

ACKNOWLEDGMENTS

The authors thank Daniel Sved and Wil Research Laboratories for their contribution to this work.

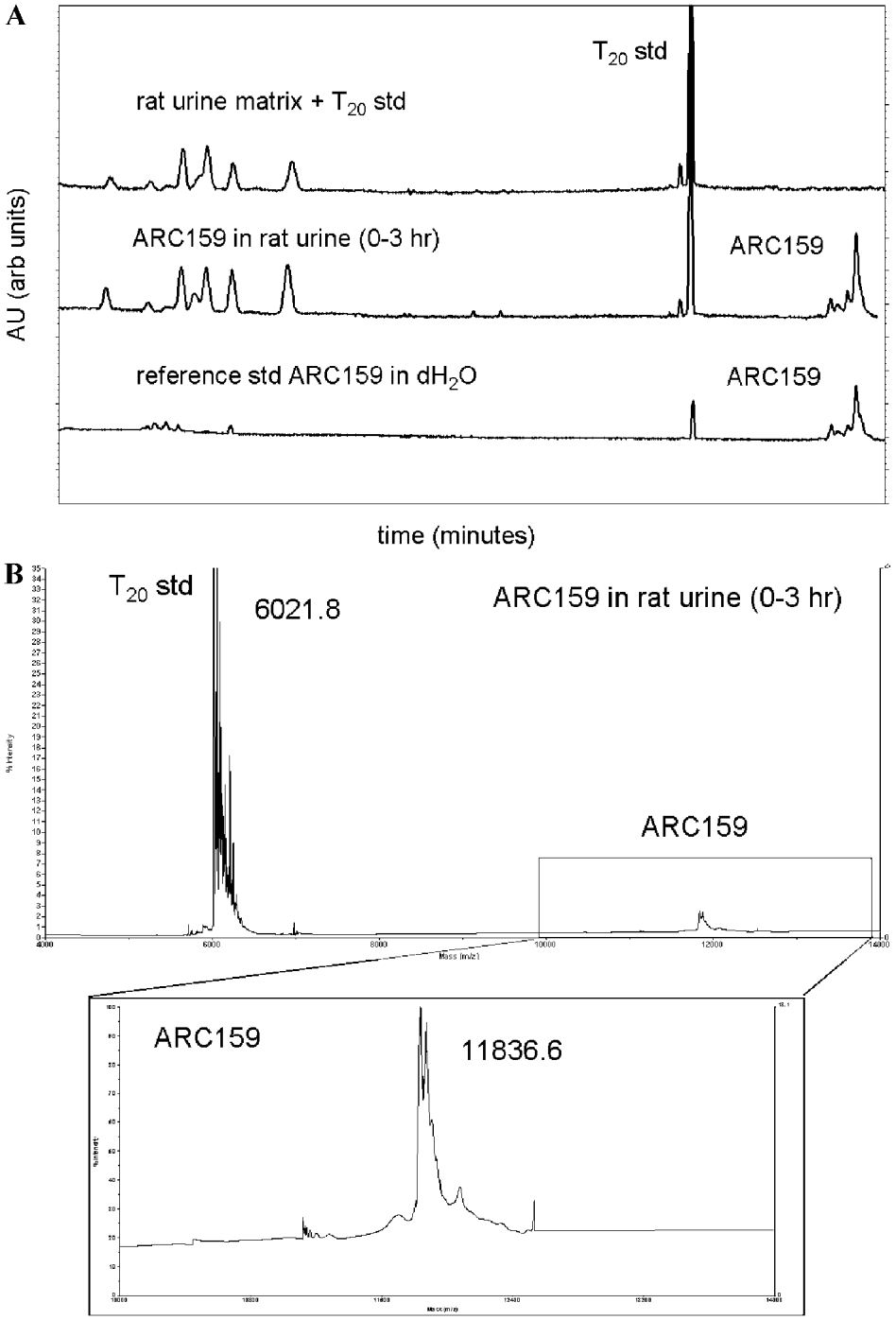

Fig. 8. Detection of full-length ARC159 aptamer in urine. Intact fully 2′-O-Me composition aptamer ARC159 was detected in urine samples from Sprague-Dawley rats (0–3 h collection interval) dosed as indicated in the legend of Fig. 4 using (A) capillary gel electrophoresis or (B) MALDI-TOF. Peaks corresponding to ARC159 and to a 20-mer internal standard are indicated.

REFERENCES

1. A. D. Ellington and J. W. Szostak. *In vitro* selection of RNA molecules that bind specific ligands. *Nature* **346**: 818–22 (1990).
2. C. Tuerk and L. Gold. Systematic evolution of ligands by exponential enrichment: RNA ligands to bacteriophage T4 DNA polymerase. *Science* **249**: 505–510 (1990).
3. R. D. Jenison, S. D. Jennings, D. W. Walker, R. F. Bargatze, and D. Parma. Oligonucleotide inhibitors of P-selectin-dependent neutrophil-platelet adhesion. *Antisense Nucleic Acid Drug Dev* **8**: 265–79 (1998).
4. L. C. Griffin, J. J. Toole, and L. L. Leung. The discovery and characterization of a novel nucleotide-based thrombin inhibitor. *Gene* **137**: 25–31 (1993).
5. S. R. Watson, Y. F. Chang, D. O'Connell, L. Weigand, S. Ringquist, and D. H. Parma. Anti-L-selectin aptamers: binding characteristics, pharmacokinetic parameters, and activity against an intravascular target *in vivo*. *Antisense Nucleic Acid Drug Dev* **10**: 63–75 (2000).
6. M. Khati, M. Schuman, J. Ibrahim, Q. Sattentau, S. Gordon, and W. James. Neutralization of infectivity of diverse R5 clinical iso-

lates of human immunodeficiency virus type 1 by gp120-binding 2′F-RNA aptamers. *J Virol* **77**: 12692–8 (2003).
7. C. H. Chen, G. A. Chernis, V. Q. Hoang, and R. Landgraf. Inhibition of heregulin signaling by an aptamer that preferentially binds to the oligomeric form of human epidermal growth factor receptor-3. *Proc Natl Acad Sci U S A* **100**: 9226–31 (2003).
8. N. K. Vaish, R. Larralde, A. W. Fraley, J. W. Szostak, and L. W. McLaughlin. A novel, modification-dependent ATP-binding aptamer selected from an RNA library incorporating a cationic functionality. *Biochemistry* **42**: 8842–51 (2003).
9. D. A. Daniels, A. K. Sohal, S. Rees, and R. Grisshammer. Generation of RNA aptamers to the G-protein-coupled receptor for neurotensin, NTS-1. *Anal Biochem* **305**: 214–26 (2002).
10. C. Bell, E. Lynam, D. J. Landfair, N. Janjic, and M. E. Wiles. Oligonucleotide NX1838 inhibits VEGF165-mediated cellular responses *in vitro*. *In Vitro Cell Dev Biol Anim* **35**: 533–42 (1999).
11. B. Wlotzka, S. Leva, B. Eschgfaller, J. Burmeister, F. Kleinjung, C. Kaduk, P. Muhn, H. Hess-Stumpp, and S. Klussmann. *In vivo* properties of an anti-GnRH Spiegelmer: an example of an oligonucleotide-based therapeutic substance class. *Proc Natl Acad Sci U S A* **99**: 8898–902 (2002).
12. L. Reyderman and S. Stavchansky. Pharmacokinetics and biodistribution of a nucleotide-based thrombin inhibitor in rats. *Pharmaceutical Research* **15**: 904–10 (1998).
13. C. E. Tucker, L. S. Chen, M. B. Judkins, J. A. Farmer, S. C. Gill, and D. W. Drolet. Detection and plasma pharmacokinetics of an anti-vascular endothelial growth factor oligonucleotide-aptamer (NX1838) in rhesus monkeys. **732**: 203–12 (1999).
14. Eyetech Study Group. Preclinical and phase 1A clinical evaluation of an anti-VEGF pegylated aptamer (EYE001) for the treatment of exudative age-related macular degeneration. *Retina* **22**: 143–52 (2002).
15. K. G. Carrasquillo, J. A. Ricker, I. K. Rigas, J. W. Miller, E. S. Gragoudas, and A. P. Adamis. Controlled delivery of the anti-VEGF aptamer EYE001 with poly(lactic-co-glycolic)acid microspheres. *Invest Ophthalmol Vis Sci* **44**: 290–9 (2003).
16. L. S. Green, D. Jellinek, C. Bell, L. A. Beebe, B. D. Feistner, S. C. Gill, F. M. Jucker, and N. Janjic. Nuclease-resistant nucleic acid ligands to vascular permeability factor/vascular endothelial growth factor. *Chem Biol* **2**: 683–95 (1995).
17. D. Jellinek, L. S. Green, C. Bell, C. K. Lynott, N. Gill, C. Vargeese, G. Kirschenheuter, D. P. McGee, P. Abesinghe, W. A. Pieken, and et al. Potent 2′-amino-2′-deoxypyrimidine RNA inhibitors of basic fibroblast growth factor. *Biochemistry* **34**: 11363–72 (1995).
18. J. Ruckman, L. S. Green, J. Beeson, S. Waugh, W. L. Gillette, D. D. Henninger, L. Claesson-Welsh, and N. Janjic. 2′-Fluoropyrimidine RNA-based aptamers to the 165-amino acid form of vascular endothelial growth factor (VEGF165). Inhibition of receptor binding and VEGF-induced vascular permeability through interactions requiring the exon 7-encoded domain. *J Biol Chem* **273**: 20556–67 (1998).
19. E. Uhlmann, A. Peyman, A. Ryte, A. Schmidt, and E. Buddecke. Use of minimally modified antisense oligonucleotides for specific inhibition of gene expression. *Methods Enzymol* **313**: 268–84 (2000).
20. P. E. Burmeister, S.D. Lewis, R.F. Silva, J.R. Preiss, L.R. Horwitz, P.S. Pendergrast, T.G. McCauley, J. C. Kurz, D. M. Epstein, C. Wilson, and A. D. Keefe. Direct *In Vitro* Selection of a 2′-*O*-Methyl-Stabilized Aptamer Against VEGF. *Chem Biol,* in press (2004).
21. J. Chelliserrykattil and A. D. Ellington. Evolution of a T7 RNA polymerase variant that transcribes 2′-*O*-methyl RNA. *Nat Biotechnol* **22**: 1155–60 (2004).
22. S. Agrawal and R. Zhang. Pharmacokinetics of oligonucleotides. *Ciba Found Symp* **209**: 60–75; discussion 75–8 (1997).
23. S. Akhtarand S. Agrawal. *In vivo* studies with antisense oligonucleotides. *Trends Pharmacol Sci* **18**: 12–8 (1997).
24. S. T. Crooke. Advances in understanding the pharmacological properties of antisense oligonucleotides. *Adv Pharmacol* **40**: 1–49 (1997).
25. J. M. Grindel, T. J. Musick, Z. Jiang, A. Roskey, and S. Agrawal. Pharmacokinetics and metabolism of an oligodeoxynucleotide phosphorothioate (GEM91) in cynomolgus monkeys following intravenous infusion. *Antisense Nucleic Acid Drug Dev* **8**: 43–52 (1998).
26. D. K. Monteith and A. A. Levin. Synthetic oligonucleotides: the development of antisense therapeutics. *Toxicol Pathol* **27**: 8–13 (1999).
27. B. Peng, J. Andrews, I. Nestorov, B. Brennan, P. Nicklin, and M. Rowland. Tissue distribution and physiologically based pharmacokinetics of antisense phosphorothioate oligonucleotide ISIS 1082 in rat. *Antisense Nucleic Acid Drug Dev* **11**: 15–27 (2001).
28. S. K. Srinivasan and P. Iversen. Review of *in vivo* pharmacokinetics and toxicology of phosphorothioate oligonucleotides. *J Clin Lab Anal* **9**: 129–37 (1995).
29. I. Lebedeva, L. Benimetskaya, C. A. Stein, and M. Vilenchik. Cellular delivery of antisense oligonucleotides. *Eur J Pharm Biopharm* **50**: 101–19 (2000).
30. M. Antopolsky, E. Azhayeva, U. Tengvall, S. Auriola, I. Jaaskelainen, S. Ronkko, P. Honkakoski, A. Urtti, H. Lonnberg, and A. Azhayev. Peptide-oligonucleotide phosphorothioate conjugates with membrane translocation and nuclear localization properties. *Bioconjug Chem* **10**: 598–606 (1999).
31. A. Astriab-Fisher, D. S. Sergueev, M. Fisher, B. R. Shaw, and R. L. Juliano. Antisense inhibition of P-glycoprotein expression using peptide-oligonucleotide conjugates. *Biochem Pharmacol* **60**: 83–90 (2000).
32. M. Manoharan. Oligonucleotide conjugates as potential antisense drugs with improved uptake, biodistribution, targeted delivery, and mechanism of action. *Antisense Nucleic Acid Drug Dev* **12**: 103–28 (2002).
33. E. M. Zubin, E. A. Romanova, E. M. Volkov, V. N. Tashlitsky, G. A. Korshunova, Z. A. Shabarova, and T. S. Oretskaya. Oligonucleotide-peptide conjugates as potential antisense agents. *FEBS Lett* **456**: 59–62 (1999).
34. P. C. de Smidt, T. Le Doan, S. de Falco, and T. J. van Berkel. Association of antisense nucleotides with lipoproteins prolongs the plasma half-life and modifies tissue distribution. *Nucleic Acids Res* **19**: 4695–4700 (1991).
35. E. Vives, P. Brodin, and B. Lebleu. A truncated HIV-1 Tat protein basic domain rapidly translocates through the plasma membrane and accumulates in the cell nucleus. *J Biol Chem* **272**: 16010–7 (1997).
36. G. A. Pietersz, W. Li, and V. Apostolopoulos. A 16-mer peptide (RQIKIWFQNRRMKWKK) from antennapedia preferentially targets the Class I pathway. *Vaccine* **19**: 1397–405 (2001).
37. J. B. Rothbard, S. Garlington, Q. Lin, T. Kirschberg, E. Kreider, P. L. McGrane, P. A. Wender, and P. A. Khavari. Conjugation of arginine oligomers to cyclosporin A facilitates topical delivery and inhibition of inflammation. *Nat Med* **6**: 1253–7 (2000).
38. J. B. Rothbard, E. Kreider, C. L. VanDeusen, L. Wright, B. L. Wylie, and P. A. Wender. Arginine-rich molecular transporters for drug delivery: role of backbone spacing in cellular uptake. *J Med Chem* **45**: 3612–8 (2002).
39. N. Pagratis, M. Lochrie, and L. Gold. High affinity TGFb nucleic acid ligands and inhibitors, Gilead Sciences, Inc., USA, 2002.
40. M. J. Graham, S. M. Freier, R. M. Crooke, D. J. Ecker, R. N. Maslova, and E. A. Lesnik. Tritium labeling of antisense oligonucleotides by exchange with tritiated water. *Nucleic Acids Res* **21**: 3737–43 (1993).
41. S. Uemura, J. B. Rothbard, H. Matsushita, P. S. Tsao, C. G. Fathman, and J. P. Cooke. Short polymers of arginine rapidly translocate into vascular cells: effects on nitric oxide synthesis. *Circ J* **66**: 1155–60 (2002).
42. B. Tavitian, S. Terrazzino, B. Kuhnast, S. Marzabal, O. Stettler, F. Dolle, J. R. Deverre, A. Jobert, F. Hinnen, B. Bendriem, C. Crouzel, and L. Di Giamberardino. *In vivo* imaging of oligonucleotides with positron emission tomography. *Nat Med* **4**: 467–71 (1998).
43. C. M. Smith and J. A. Steitz. Sno storm in the nucleolus: new roles for myriad small RNPs. *Cell* **89**: 669–72 (1997).
44. F. C. Richardson, R. D. Kuchta, A. Mazurkiewicz, and K. A. Richardson. Polymerization of 2′-fluoro- and 2′-*O*-methyl-dNTPs by human DNA polymerase alpha, polymerase gamma, and primase. *Biochem Pharmacol* **59**: 1045–52 (2000).
45. F. C. Richardson, C. Zhang, S. R. Lehrman, H. Koc, J. A. Swenberg, K. A. Richardson, and R. A. Bendele. Quantification of 2′-fluoro-2′-deoxyuridine and 2′-fluoro-2′-deoxycytidine in DNA and RNA isolated from rats and woodchucks using LC/MS/MS. *Chem Res Toxicol* **15**: 922–6 (2002).
46. R. S. Geary, T. A. Watanabe, L. Truong, S. Freier, E. A. Lesnik, N. B. Sioufi, H. Sasmor, M. Manoharan, and A. A. Levin. Pharmacokinetic properties of 2′-*O*-(2-methoxyethyl)-modified oligonucleotide analogs in rats. *J Pharmacol Exp Ther* **296**: 890–7 (2001).